Nanocomposite electrolytes for lithium batteries with reduced flammability

Apostolos Enotiadis [a], Nikhil J. Fernandes [b], Natalie A. Becerra [a], Mauro Zammarano [c], Emmanuel P. Giannelis [a, *]

[a] Department of Materials Science and Engineering, Cornell University, Ithaca, NY 14853, USA
[b] School of Applied and Engineering Physics, Cornell University, Ithaca, New York 14853, USA
[c] Flammability Reduction Group Engineering Laboratory, National Institute of Standards and Technology, 100 Bureau Drive, Gaithersburg, MD 20899-8665, USA

ABSTRACT

We report a family of flame-retardant electrolytes for lithium batteries based on ionic nanocomposites. The nanocomposites are synthesized in one pot by dispersing SiO_2 nanoparticles charge-balanced by both Li ions and mono-amino-terminated polyether (PEO-*b*-PPO-NH$_3^+$) in an oligomeric PEO matrix. The Li^+ and PEO-*b*-PPO-NH$_3^+$ ions lead to enhanced Li^+ transference number and compatibility with the PEO matrix, respectively. The nanocomposite electrolyte containing 40% mass fraction of silica shows a notable electrochemical stability window of more than 6 V in contact with Lithium and high Li^+ transference number over 0.5. Rheology measurements demonstrate the tunability of the system from liquid to gel-like as the silica mass fraction percentage increases from 0 to 40% while the conductivity remains almost constant. Thermal gravimetric and microscale combustion calorimeter measurements of the nanocomposites show decreased rate of mass loss and heat release rate compared to neat electrolyte. Finally, the fire retardancy of the nanocomposites measured by directly observing the formation and sustainability of flame, when exposed to direct fire, make them promising candidates in the ever-growing quest for safe lithium batteries.

© 2018 Elsevier Ltd. All rights reserved.

1. Introduction

Interest in lithium batteries has been growing in the last decade due to their significance in various portable electronic devices and electric vehicles [1, 2] In addition to the other components, the role of the electrolyte has also become critical for ensuring good battery performance. The electrolyte needs to meet a series of requirements including high ionic conductivity, high transference number of lithium ions, chemical and thermal stability, high mechanical strength and ease of processing to create high-performance batteries [3,4]. Recently, increased attention has been given to the flammability resistance of electrolytes in order to avoid any potential fire hazard in various types of accidents [5,6].

Polyethylene oxide, (PEO) is one of the most widely researched and most attractive polymer electrolytes for several classes of advanced lithium batteries [7–9]. PEO displays excellent solvation and complexing ability towards alkali metal ions such as lithium. In recent years, substantial interest has been devoted to developing solvent-free electrolytes using neat moderate/low molar mass PEGs (poly ethylene glycol), for highly conductive gels [10–12]. However, mechanical properties, long-term stability, and low ignition temperature remain an issue.

A common strategy to improve the mechanical and electrochemical properties of polymer electrolytes is the incorporation of inorganic particles [1,10,13,14]. In several systems, the inorganic particles enhance the segmental motion of the host polymer acting as solid plasticizers thus increasing ion conduction while improving at the same time the mechanical properties of the electrolyte. However, particle dispersion in the polymer matrix is a challenging task that has prevented nanocomposites from reaching their true potential. To that end, our group has introduced *ionic* nanocomposite systems consisting of a polymeric canopy bound to a well-defined nanoparticle core by ionic interactions [15,16]. Due to the ionic interactions present, the perennial dispersion challenges associated with conventional nanocomposites void of

---

specific interactions are minimized while the dynamic nature of the ionic bonds provides opportunities for adaptive/multi-responsive properties.

The incorporation of inorganic particles in several polymers can also improve thermal resistance and flame retardancy [17,18]. Kashiwagi [19] et al., for example, studied the flame retardancy of various types of silica/polyethylene oxide hybrids. They found that addition of silica leads to the formation of strong char/silica surface layers acting as thermal insulation and barrier protecting the PEO against the migration of thermal degradation products to the surface.

Building on the ionic motif Schaefer [20] et al., Liu [14] et al. and Lee [21] et al. reported a series of single-ion electrolytes based on lithium-exchanged sulfonated silica nanoparticles. In both cases, surface modification of the silica nanoparticles with sulfonated silane to endow the particles with ionic groups was required. Our group reported an alternative approach to synthesize ionic nanocomposites by exploiting the acid/base properties of bare SiO_2 particles. By reacting directly, the inherently acidic hydroxyl groups of silica nanoparticles with an end-functionalized amine-PEG (PEG-NH_2) leads to nanocomposites with an excellent dispersion of the nanoparticles.

In this paper, we integrate the need of good dispersion with high ionic conductivity/high transference number to demonstrate a new family of nanocomposite electrolytes. The nanocomposites are synthesized in one pot by dispersing SiO_2 nanoparticles charge-balanced by both Li ions and PEO-*b*-PPO-NH_3^+ in an oligomeric PEO matrix (Fig. 1). The Li^+ ions on the silica provide enhanced ionic conductivity and higher transference number while the short PEO-b-PPO-NH_3^+ chains enhance the compatibility with the PEO matrix. In addition to the enhanced electrochemical and thermal stability, the nanocomposite electrolytes containing 40% by mass of silica show remarkable resistance to open-flame ignition.

2. Experimental[1]

Materials. Silica nanoparticles (LUDOX HS30 colloidal silica, 30% mass fraction suspension in H_2O, 16–18 nm diameter), lithium hydroxide monohydrate ($\geq$98.0%), Dowex HCR-W2 ion-exchange resin, bis(trifluoromethane)sulfonimide lithium salt (99.95% trace metals basis) and poly(ethylene glycol) methyl ether (average Mn 550) were obtained from Aldrich Chemical Company. Jeffamine® M-2070 polyether amine, composed of block of polypropylene oxide and polyethylene oxide oligomers (PPO-*b*-PEO-NH_2) was received from Huntsman Corporation (The Woodlands, TX). All materials were used as supplied.

Synthesis of Electrolytes. HS30 silica suspension is first diluted to 3 wt % and passed three times through a column of proton-exchanged Dowex resin to produce silica with fully protonated surface hydroxyls, (HS30)-OH. Then a stoichiometric amount of LiOH and PPO-*b*-PEO-NH2 (in 50/50 M ratio) to fully neutralize the acid sites was added while specific amounts of PEG matrix (550 mol/g) was added in the end to create the various mass silica fractions (0, 10, 20, 25, 30 and 40%) in one pot synthesis. The amount of PPO-*b*-PEO-NH_2/LiOH was determined by first titrating a known volume of 3 wt % (HS30)-OH solution with a 1 mmol/L NaOH

solution and monitoring the pH. The suspension was stirred vigorously for about 6 h before it was frozen with liquid nitrogen and then placed in a lyophilizer to remove the water. Then, the sample was dried at 45 °C in vacuum for 48 h and placed in a glove box. Finally, bis(trifluoromethane)sulfonimide lithium salt added to the electrolytes to keep EO/Li = 50 ratio taking account the immobilized Li-ions on the silica particles surfaces especially in the case of the nanocomposite electrolytes. The final ionic electrolytes denoted hereafter as IE_X%, where X is the silica mass fraction.

Characterization. TGA and DSC measurements were obtained on a TA Instruments model Q5000 and TA Instruments model Q2000, respectively under air flow. The amount of crystalline PEO (% wt) was calculated using the following equation [22]:
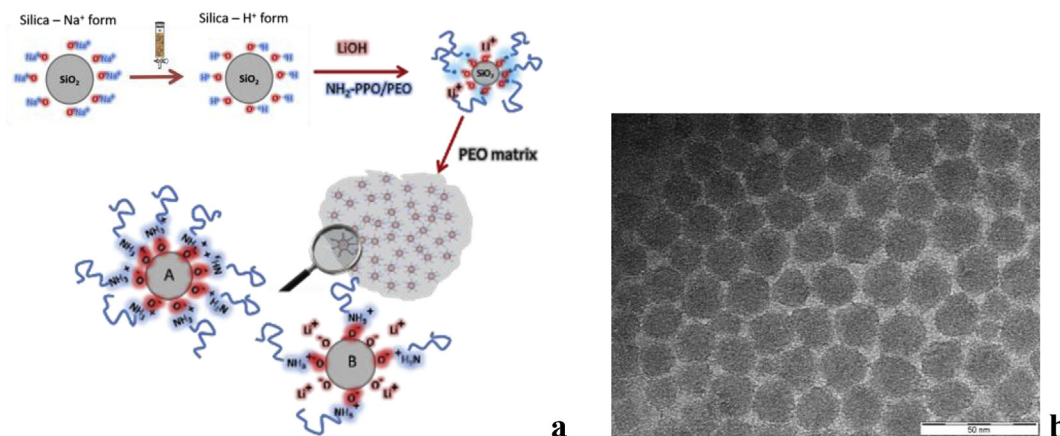
$$K = \frac{\Delta H_c}{(1-a) \cdot \Delta H_o}$$

where ΔH_c is the apparent heat of fusion per gram of the sample, α is the concentration of silica nanoparticles in wt %, and ΔH_o is the thermodynamic heat of fusion per gram of 100% crystalline PEO [23].

Dielectric measurements were performed on a Novacontrol model N40 dielectric broadband spectrometer. The ionic conductivity was measured by AC impedance spectroscopy in the frequency range from 100 KHz to 1 Hz at temperatures between −10 °C and 80 °C [24]. For electron microscopy, the samples were diluted to 1% by mass in deionized water, and then a 5 μL drop was placed on a copper grid and allowed to rest for a minute before most of the water was blotted away. The grid was dried completely in the air. Bright-field TEM was carried out on an FEI Tecnai T12 microscope operating at 120 kV. Rheological measurements were conducted on an Anton Paar MCR-501 rheometer equipped with a 25 mm diameter cone and plate geometry (measuring system CP25-1). Electrochemical properties were measured using a Swagelok assembly by sandwiching the electrolyte between stainless steel cells and lithium metal as a counter electrode at 25 °C on Solartron Electrochemical Impedance Spectrometer. Polypropylene (PP) separator or donut shaped Teflon ring was used to prevent any short circuit of a symmetrical coin cell battery. Transference numbers were determined at room temperature according to the polarization method proposed by Bruce and Scrosati [25,26] using a Solartron Potentiostat (with a step of 3 mV) and a Solartron Frequency Response Analyzer. The test was repeated three times and the reported value is the average with a standard deviation of ±0.1. The electrochemical window was measured by linear scan sweep voltammetry at a scan rate of 1 mV/ s also performed at room temperature.

The flammability of the electrolytes was evaluated first by observing the formation of flame when exposed to direct fire, as described in the literature [27,28]. More specifically, we use a naphtha-type lighter with a ≈ 1 cm flame size. In the case of liquid-like electrolytes in which the use of a separator membrane is necessary, we bring the flame to a distance of 1 cm–2 cm from the sample while for the free-standing, gel-like sample, the flame comes in direct contact with the sample. Microscale combustibility experiments were carried out in a Govmark MCC-1 microscale combustion calorimeter. The specimens were first kept at 100 °C for 5 min to remove adsorbed moisture and then heated up to 600 °C at a heating rate of 1 °C/s, in a stream of nitrogen flowing at 80 cm^3/ min. The pyrolysis volatiles released from the thermal degradation of the sample into the nitrogen gas stream were mixed with a 20 cm^3/min stream of pure oxygen prior to entering a 900 °C combustion furnace. Three samples weighing about 5 mg were tested for each system. The amount of residue is calculated by weighing the sample before and after testing.

Fig. 1. a) Schematic showing the synthesis of nanocomposite ionic electrolytes and b) TEM image of silica nanoparticles anchoring Li ions and amino terminated polyethers in 50/50 M ratio.

3. Results and discussion

Fig. 1a shows a schematic of the synthesis of the nanocomposite electrolytes, where we exploit the inherent acidity/ion exchange properties of the native hydroxyl groups on the silica. The process involves passing first commercially available colloidal silica particles through a proton exchange resin. The protonation of the silica particles is critical for the subsequent acid/base chemistry, where simultaneous reaction with LiOH and the amino terminated PPO-*b*-PEO-NH$_2$ forms particles bearing a random distribution of both. The second step involves adding the functionalized silica particles to the PEO matrix. The stoichiometric amount of LiOH and PPO-*b*-PEO-NH$_2$ was determined from the inflection point in a titration curve using NaOH solution. The PPO-*b*-PEO-NH$_2$ compatibilizes the silica particles with the PEO matrix while the Li ions contribute to the ionic conductivity and lead to increased cation transference number (vide infra). In the absence of PPO-*b*-PEO-NH$_2$, the silica particles phase-separate in the final electrolyte leading to a non-uniform system while low conductivity/low Li transference number electrolytes are obtained, when LiOH is not used.

Fig. 1b shows a TEM image of silica nanoparticles with a 50% of the total number of surface hydroxyl groups neutralized by the amino-terminated PPO-*b*-PEO. The size of particles obtained from the TEM is ≈ 20 nm and is consistent with the size obtained from DLS measurements (22 nm in water). Thus the ionic interactions of the silica with the amine groups of the PPO-*b*-PEO oligomer contribute to the stabilization and dispersion of the silica particles [29,30].

3.1. Flammability

As fire accidents from batteries are quite dangerous and can cause emission of toxic gases, ignition resistance has become an essential requirement for practical applications of Li batteries. Table 1 shows screenshots from videos obtained by subjecting the neat and nanocomposite electrolytes after exposure to direct flame. Note that, since the electrolytes containing (0 and 20) wt. % silica are liquid-like they were tested with a polypropylene, PP, membrane separator (9-10 drops were added to the separator prior to testing). In contrast, the 40 wt % silica electrolyte is gel-like and self-supported. Therefore, it was tested by itself (without the need of the PP separator). The neat PEO electrolyte (0 wt% silica) was highly flammable and easily ignited in less than a second, after exposure to flame. A significant reduction in flammability with self-extinguishing behavior was observed for the also liquid-like
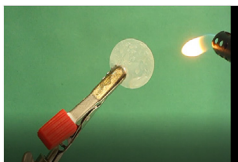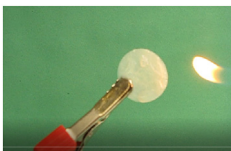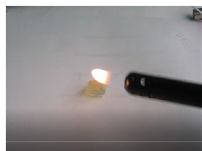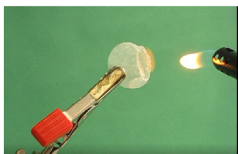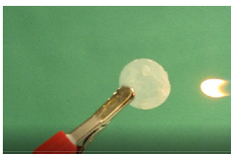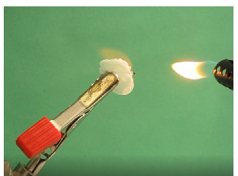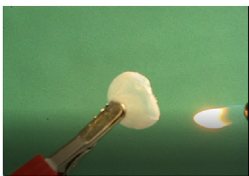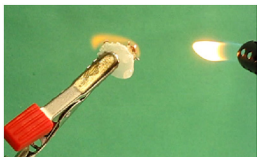
nanocomposite electrolyte containing 20 wt % silica nanoparticles. This sample ignited in about 9 s from flame impingement when the flame approached within a distance of 1 cm–2 cm from the sample, and self-extinguished in about 11 s after removal of the ignition flame. Finally, the 40 wt % silica nanocomposite shows improved ignition resistance as shown by absence of sample ignition even after repeated exposure and direct contact with the flame. As we mentioned above the high silica content leads to gel- or solid-like behavior thus eliminating the need for a separator. Note that the removal of a flammable PP separator might contribute to the improved performance of the 40 % wt. sample as compared to the 20 wt % sample.

Fig. 2 compares the thermogravimetric analysis of the nanocomposite electrolyte containing 40 wt % silica to the neat electrolyte. The temperature at which 50% mass loss occurs, increases from 409 °C to 455 °C in the case of the 40 wt % silica containing nanocompos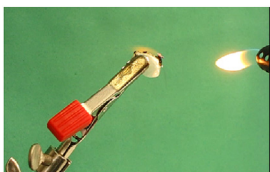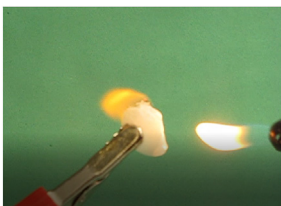ite electrolyte showing an improvement in thermal stability and indicating a slower rate of PEO combustion. Moreover, the residue amount increases from (2–44) wt. % compared to the neat electrolyte because of the presence of silica nanoparticles and a small char product created during the combustion process (see Fig. 3).

The thermal stability and flammability of the samples were also evaluated by microscale combustion calorimetry, MMC. MCC simulates the burning process by using anaerobic pyrolysis and a subsequent reaction of the volatile pyrolysis products with oxygen under high temperatures to simulate surface gasification and flaming combustion. Both heat release rate and temperature as a function of time at constant heating rate are measured during the test. Key comparison parameters from the test include temperature at maximum heat release rate (T_p), heat release capacity (HRC), obtained by dividing the heat release rate at each point in time by the initial sample mass and heating rate, and total heat release (THR) from combustion of the fuel gases per unit mass of sample (obtained by time-integration of HRR over the entire test). HRC is a material property that is often used to screen the flammability of polymers when only research quantities are available for testing, making other tests not feasible [31].

The results from the MCC tests are summarized in Table 2. The residues from silica-containing electrolyte samples (20 and 40) wt. % are higher than those from the unfilled, neat electrolyte. This is consistent with the TGA results discussed previously. The values of residue indicate that silica does not induce any additional charring in the polymer and the residue is fully inorganic. In addition, as shown in Table 2, the total heat release, THR, decreases by ≈ 18%

Table 1
Summary of flammability tests.

Time (sec)	IE_0%	IE_20%	IE_40%
0			
1			
4			
6			
9			
12			

and 38% for the (20 and 40) wt% silica, respectively. The addition of silica leads to a significant reduction in the rate of release of combustible volatiles, resulting in lower flammability (as evidenced by lower total heat release, THR and heat release capacity, HRC). For example, a 38% and 25% reduction in THR and HRC compared to the neat electrolyte were observed for the nanocomposite containing 40% silica. An increase in the temperature at maximum heat release rate (T_p) is also observed in the nanocomposites. In general, an increase in T_p delays the ignition and flame spread over the material. The increased residue produced by thermal degradation in the nanocomposites could act as a protective barrier capable of reducing the heat release rate significantly. For example, a reduction in the peak of heat release between 50% and 75% was observed by Kashiwagi et al., when a percolated network of nanoparticles is present in a polymer matrix. It is possible that the present tests using MCC are underestimating the actual reduction of HRR due to the extremely small scale of the test (≈ 5 mg) at which heat/mass transfer phenomena cannot be captured.

There are concerns about the gas toxicity of electrolytes in lithium batteries [32]. An added advantage of the nanocomposite electrolytes is that the amount and release rate of toxic, combustible gasses is reduced by partially replacing toxic bis(trifluoromethane)sulfonimide lithium salt with inert lithiated silica.

3.2. Electrochemical performance

Encouraged by the improved thermal stability and flame retardancy, we next evaluated the electrochemical performance of the nanocomposite electrolytes and compared them to the neat polymer electrolyte.
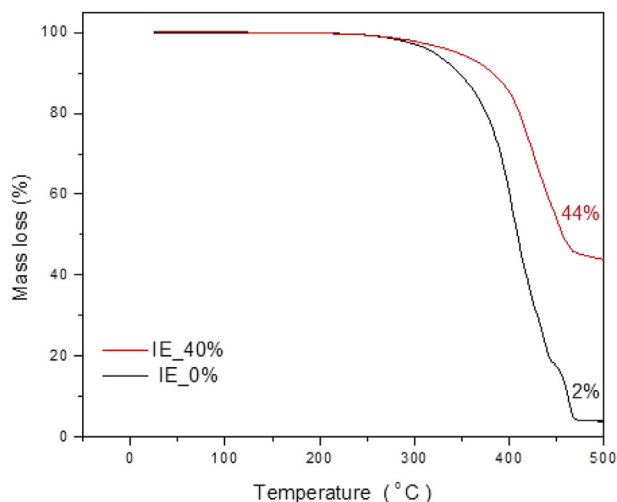
Fig. 2. TGA of neat electrolyte, and nanocomposite electrolyte containing 40 wt% silica.
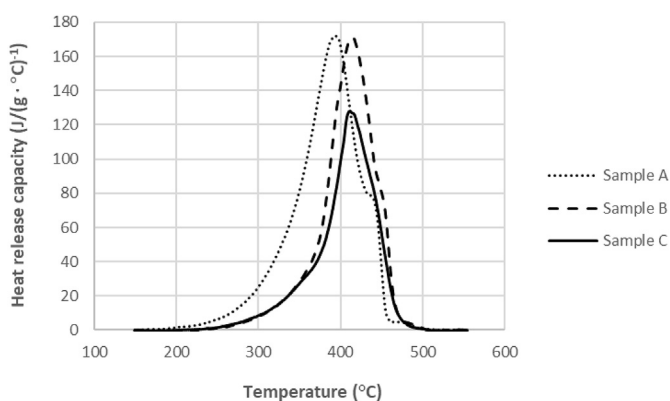

Fig. 3. Heat release capacity as a function of temperature of neat electrolyte, IE_0%, sample A, IE_25% sample B and IE_40% sample C.

Table 2
Summary of MCC Measurements (uncertainty is equal to ± one standard deviation).

Sample	Residue (%)	Tp (°C)	HRC (J/(g · °C)$^{-1}$)	THR (kJ/g)
IE_0%	0.3 ± 0.3	392 ± 2	171 ± 7	15.4 ± 0.2
IE_20%	16.1 ± 0.5	411 ± 3	170 ± 4	12.6 ± 0.3
IE_40%	37.1 ± 0.5	412 ± 1	129 ± 1	9.6 ± 0.2

Fig. 4a shows an Arrhenius plot of the ionic conductivity of all electrolytes with various silica loading. It is well known that PEO electrolytes show a transition from crystalline to the amorphous state upon heating, which is accompanied by an increase in ionic conductivity. This transition depends on the molecular weight of the PEO. As shown in Fig. 4a, for the PEO used in this work the transition takes place at room temperature. Below the melting transition, the ionic conductivity drops precipitously by several orders of magnitude ($\approx 10^{-7}$ S/cm). Consistent with previous reports the ionic conductivity of the nanocomposites for temperatures above the melting transition decreases with increasing silica content. Nevertheless, below the melting transition, all nanocomposites show significantly higher conductivity compared to the neat PEO. The increase in conductivity below the melting transition by the addition of nanoparticles has been attributed previously to the "solid plasticizing effect" [33,34], which leads to increases in the amorphous polymer fraction in the nanocomposites (as shown in Fig. 4b). Fig. 4b compares the degree of crystallization for the nanocomposites compared to the neat PEO. The amount of polymer crystallinity decreases almost linearly as the silica content increases. For the sample containing 40% silica, the amount of crystallinity decreases sharply to $\approx 9\%$. The PEO chains in the matrix are thoroughly jammed by the presence of silica nanoparticles acting as obstacles for the crystallization of PEO.

Fig. 5a shows the storage, G′, and loss, G″, moduli of the nanocomposites with various SiO$_2$ loadings as a function of shear frequency, ω. The nanocomposite with 10 wt % silica behaves as a typical liquid with G″ > G′. As the silica loading increases to 30 wt%, the storage modulus increases by more than four orders of magnitude. The loss modulus is lower than the storage modulus and showing weaker frequency dependence over the entire frequency range, which is indicative of a gel-like response (G′ > G″) [35–37]. Fig. 5b juxtaposes the ionic conductivity at room temperature with the viscosity for various systems. While the addition of silica particles has a dramatic effect on the viscosity turning them from liquid–like to gel-like, the ionic conductivity remains virtually constant at $\approx 10^{-4}$ S/cm. The ability to control the behavior from liquid-like to solid-like by varying the amount of silica with negligible changes in ionic conductivity is particularly advantageous as the high modulus can eliminate potentially dendrite formation during the battery operation.

Electrochemical stability measurements were conducted in a symmetric, lithium/electrolyte/lithium configuration in Swagelok cells. Fig. 6a shows the electrochemical stability window for the nanocomposite nanocomposite (40 wt % silica) and neat electrolyte in contact with lithium metal. The inclusion of the silica nanoparticles does improve the electrochemical robustness of the electrolyte to more than 6 V in contact with Lithium metal. Fig. 6b shows the lithium transference number for various electrolyte systems as a function of silica. The transference number was measured by a combination of AC impedance and DC polarization using the Bruce/Scrosati method as described in the experimental section. According to the literature, addition of particles in PEO generally leads to an increase in the transference number but not more than 0.5 [10,20]. In our case, the lithiated silica particles not only provide additional lithium ions but because of the negligible mobility of the silica cores are strongly increasing the cation transference number. As shown in Fig. 6b, the lithium transference number of neat PEO is 0.23, which is in agreement with previously published results [34]. The transference number, TLi$^+$, reaches 0.56 for the 40 wt% silica nanocomposite. The importance of using partially lithiated silica particles in the nanocomposites is demonstrated in Fig. 4b. The Figure compares the TLi$^+$ for electrolytes containing (20 and 40) wt% SiO$_2$ fully modified with PPO-b-PEO-NH$_2$ (red symbols). In these electrolytes, all the Li ions come from the TSFI salt. In both cases, the TLi$^+$ is lower compared to the nanocomposites synthesized using the partially lithiated silica particles. Finally, galvanotactic polarization measurements were conducted to estimate the short circuit times (Tsc) using constant current density J = 0.0354 mA/cm^{-2} of the hybrid electrolyte IE_40% in symmetrical coin cells. The Tsc for the sample containing 40 wt% is 106 h (see supporting information, S1) which is a high value compared with literature [20] giving the opportunity to improve the operation time of cell battery at a high level current density.
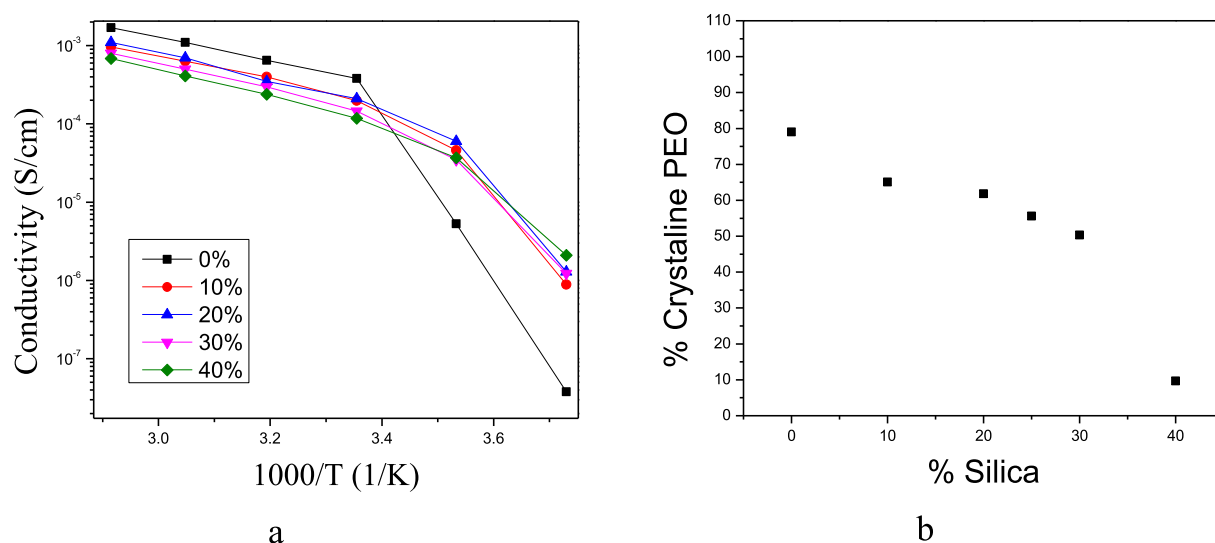
Fig. 4. a) DC ionic conductivity of electrolytes with varying silica loading compared with the neat PEO electrolyte, and b) mass fraction percentage of crystalline PEO as a function of silica loading in the nanocomposite electrolytes.
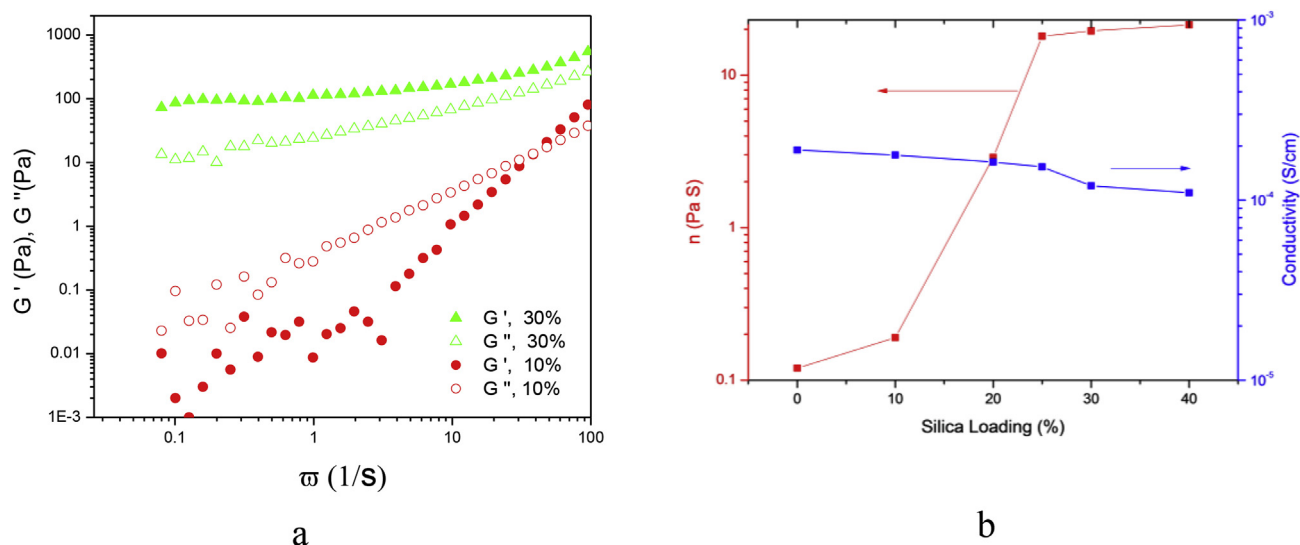
Fig. 5. a) storage modulus, G′, (filled symbols) and loss modulus, G″, (open symbols) of the electrolyte with (10 and 30) wt % silica, as a function of shear frequency and b) intrinsic viscosity and conductivity of electrolytes as a function of silica loading.
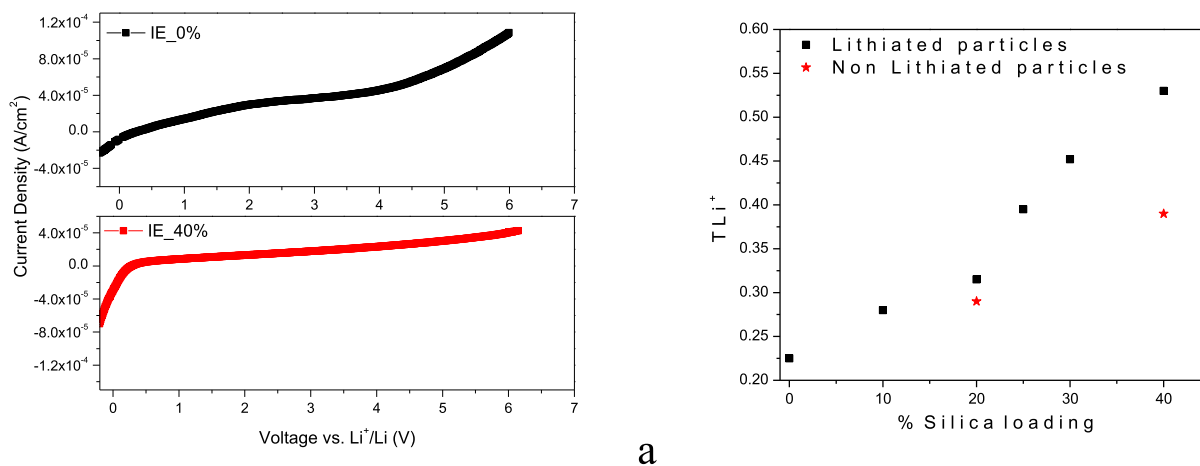
Fig. 6. a) Electrochemical windows of nanocomposite electrolyte containing 40% silica and neat electrolyte as measured in a symmetric coin cell configuration and b) Lithium transference number as a function of silica loading.

4. Conclusions

We report a simple and scalable method to synthesize well-dispersed nanocomposite electrolytes by leveraging the acid/base interactions of the surface hydroxyls on silica. Reacting hydroxylated silica nanoparticles with both LiOH and the amino terminated PPO-b-PEO-NH$_2$ leads to silica bearing a random distribution of both. The PPO-b-PEO-NH$_2$ compatibilizes the silica particles with the PEO matrix in the electrolyte while the Li ions contribute to the ionic conductivity and lead to increased cation transference number. In the absence of PPO-b-PEO-NH$_2$, the silica particles phase separates in the final electrolyte leading to a non-uniform system.

Thermal analysis and flammability measurements indicate that the nanocomposite electrolytes decrease the rate of mass loss and heat release rate, and exhibit open-flame ignition resistance in the test conditions used in this work. The nanocomposite electrolytes also suppress the amount of toxic gasses released during combustion by partially replacing toxic bis(trifluoromethane)sulfonimide lithium salt with inert lithiated silica.

The addition of silica particles has a dramatic effect on the viscosity/modulus of the materials. The nanocomposites turn from liquid−like (0−20 wt% silica) to gel-like ($\geq$30 wt%) while at the same time the ionic conductivity remains virtually constant at $\approx 10^{-4}$ S/cm. The ability to control the behavior from liquid-like to solid-like by varying the amount of silica with negligible changes in ionic conductivity is particularly advantageous as the high modulus could minimize the formation of dendrites during charge/discharge of the battery. Finally, the electrochemical stability of the nanocomposite electrolytes is improved significantly while more than doubling the lithium transference number (TLi$^+$ = 0.23 and 0.56 for the neat PEO and nanocomposite electrolyte containing 40 wt% SiO2, respectively).

Acknowledgements

Appendix A. Supplementary data

Supplementary data related to this article can be found at https://doi.org/10.1016/j.electacta.2018.02.079.

References

[1] P.G. Bruce, B. Scrosati, J.-M. Tarascon, Nanomaterials for rechargeable lithium batteries, Angew Chem. Int. Ed. Engl. 47 (2008) 2930−2946.
[2] J.B. Goodenough, K. Park, The Li-Ion rechargeable battery: a perspective the Li-Ion rechargeable battery: a perspective, J. Am. Chem. Soc. 135 (2013) 1167−1176.
[3] E. Quartarone, P. Mustarelli, Electrolytes for solid-state lithium rechargeable batteries: recent advances and perspectives, Chem. Soc. Rev. 40 (2011) 2525.
[4] B. Scrosati, J. Garche, Lithium batteries: status, prospects and future, J. Power Sources 195 (2010) 2419−2430.
[5] S. Hess, M. Wohlfahrt-Mehrens, M. Wachtler, Flammability of Li-Ion battery electrolytes: flash point and self-extinguishing time measurements, J. Electrochem. Soc. 162 (2015) A3084−A3097.
[6] K. Xu, Nonaqueous liquid electrolytes for lithium-based rechargeable batteries, Chem. Rev. 104 (2004) 4303−4417.
[7] H. Kao, S. Chao, P. Chang, Multinuclear solid-state NMR, self-diffusion coefficients, differential scanning calorimetry, and ionic conductivity of solid organic - inorganic hybrid electrolytes based on PPG - PEG - PPG diamine, siloxane, and lithium perchlorate, Macromolecules 39 (2006) 1029−1040.
[8] H.-M. Kao, C.-L. Chen, An organic-inorganic hybrid electrolyte derived from self-assembly of a poly(ethylene oxide)-poly(propylene oxide)-poly(ethylene oxide) triblock copolymer, Angew Chem. Int. Ed. Engl. 43 (2004) 980−984.
[9] A.M. Stephan, Review on gel polymer electrolytes for lithium batteries, Eur. Polym. J. 42 (2006) 21−42.
[10] J. Zhou, Ionic conductivity of composite electrolytes based on oligo(ethylene oxide) and fumed oxides, Solid State Ionics 166 (2004) 275−293.
[11] D. Swierczynski, A. Zalewska, W. Wieczorek, Composite polymeric electrolytes from the PEODME - LiClO 4-SiO 2 system, Chem. Mater. 13 (2001) 1560−1564.
[12] B.J.L. Nugent, S.S. Moganty, L.A. Archer, Nanoscale organic hybrid electrolytes, Adv. Mater. 5201 (2010) 3677−3680.
[13] S.K. Chaurasia, A. Chandra, Organic-inorganic hybrid electrolytes by in-situ dispersion of silica nanospheres in polymer matrix, Solid State Ionics 307 (2017) 35−43.
[14] Z. Jia, W. Yuan, H. Zhao, H. Hu, G.L. Baker, Composite electrolytes comprised of poly(ethylene oxide) and silica nanoparticles with grafted poly(ethylene oxide)-containing polymers, RSC Adv. 4 (2014) 41087−41098.
[15] N.J. Fernandes, J. Akbarzadeh, H. Peterlik, E.P. Giannelis, Terms of use synthesis and properties of highly dispersed ionic silica À poly (ethylene oxide) nanohybrids, ASC Nano (2013) 1265−1271.
[16] L.G. Boutsika, A. Enotiadis, I. Nicotera, C. Simari, G. Charalambopoulou, E.P. Giannelis, T. Steriotis, Nafion® nanocomposite membranes with enhanced properties at high temperature and low humidity environments, Int. J. Hydrogen Energy 41 (2016) 22406−22414.
[17] J. Li, P. Wei, L. Li, Y. Qian, C. Wang, N.H. Huang, Synergistic effect of mesoporous silica SBA-15 on intumescent flame-retardant polypropylene, Fire Mater. 35 (2011) 83−91.
[18] L. Ye, Q. Wu, B. Qu, Synergistic effects of fumed silica on intumescent, J. Appl. Polym. Sci. 115 (2011) 3508−3515.
[19] T. Kashiwagi, J.W. Gilman, K.M. Butler, R.H. Harris, J.R. Shields, A. Asano, Flame retardant mechanism of silica gel/silica, Fire Mater. 24 (2000) 277−289.
[20] J.L. Schaefer, D.A. Yanga, L.A. Archer, High lithium transference number electrolytes via creation of 3-dimensional, charged, nanoporous networks from dense functionalized nanoparticle composites, Chem. Mater. 25 (2013) 834−839.
[21] Y.-S. Lee, S.H. Ju, J.-H. Kim, S.S. Hwang, J.-M. Choi, Y.-K. Sun, H. Kim, B. Scrosati, D.-W. Kim, Composite gel polymer electrolytes containing core-shell structured SiO2(Li+) particles for lithium-ion polymer batteries, Electrochem. Commun. 17 (2012) 18−21.
[22] S. Jiang, C. Qiao, S. Tian, X. Ji, L. An, B. Jiang, Confined crystallization behavior of PEO in organic networks, Polymer 42 (2001) 5755−5761.
[23] Z. Mo, K.B. Lee, Y.B. Moon, M. Kobayashi, A.J. Heeger, F. Wudl, X-ray scattering from polythiophene: crystallinity and crystallographic structure, Macromolecules 18 (1985) 1972−1977.
[24] A.K. Johnsker, © 1977 nature publishing group, Nature 267 (1977) 673.
[25] P.G. Bruce, J. Evans, C.A. Vincent, Conductivity and Transference Number Measurements on polymer electrolytes, Solid State Ionics 28−30 (1988) 918−922.
[26] G.B. Appetecchi, G. Dautzenberg, B. Scrosati, A new class of advanced polymer electrolytes and their relevance in plastic-like, rechargeable lithium batteries, J. Electrochem. Soc. 143 (1996) 6.
[27] I. Quinzeni, S. Ferrari, E. Quartarone, C. Tomasi, M. Fagnoni, P. Mustarelli, Li-doped mixtures of alkoxy-N-methylpyrrolidinium bis(trifluoromethanesulfonyl)-imide and organic carbonates as safe liquid electrolytes for lithium batteries, J. Power Sources 237 (2013) 204−209.
[28] L. Lombardo, S. Brutti, M.A. Navarra, S. Panero, P. Reale, Mixtures of ionic liquid − alkylcarbonates as electrolytes for safe lithium-ion batteries, J. Power Sources 227 (2013) 8−14.
[29] N.J. Fernandes, J. Akbarzadeh, H. Peterlik, E.P. Giannelis, Synthesis and properties of highly dispersed ionic silica-poly(ethylene oxide) nanohybrids, ACS Nano 7 (2013) 1265−1271.
[30] R.R. Madathingal, S.L. Wunder, Confinement effects of silica nanoparticles with radii smaller and larger than rg of adsorbed poly(ethylene oxide), Macromolecules 44 (2011) 2873−2882.
[31] T.S. Lin, J.M. Cogen, R.E. Lyon, Correlations between microscale combustion calorimetry and conventional flammability tests for flame retardant wire and cable compounds, in: Proc. 56th IWCS, 2007, pp. 176−185.
[32] N.P. Lebedeva, L. Boon-Brett, Considerations on the chemical toxicity of contemporary Li-Ion battery electrolytes and their components, J. Electrochem. Soc. 163 (2016) A821−A830.
[33] F. Croce, G.B. Appetecchi, L. Persi, B. Scrosat, Nanocomposite polymer electrolytes for lithium batteries, Nature 394 (1998) 456.
[34] F. Croce, S. Sacchetti, B. Scrosati, Advanced, high-performance composite polymer electrolytes for lithium batteries, J. Power Sources 161 (2006) 560−564.
[35] J.L. Schaefer, S.S. Moganty, D.A. Yanga, L.A. Archer, Nanoporous hybrid electrolytes, J. Mater. Chem. 21 (2011) 10094.
[36] H.J. Walls, M.W. Riley, R.R. Singhal, R.J. Spontak, P.S. Fedkiw, S.A. Khan, Nanocomposite electrolytes with fumed silica and hectorite clay networks: passive versus active fillers, Adv. Funct. Mater. 13 (2003) 710−717.
[37] P. Sollich, F. Lequeux, P. Hébraud, M.E. Cates, Rheology of soft glassy materials, Phys. Rev. Lett. 78 (1997) 2020−2023.